Adsorption of the Xanthan Gum Polymer and Sodium Dodecylbenzenesulfonate Surfactant in Sandstone Reservoirs: Experimental and Density Function Theory Studies

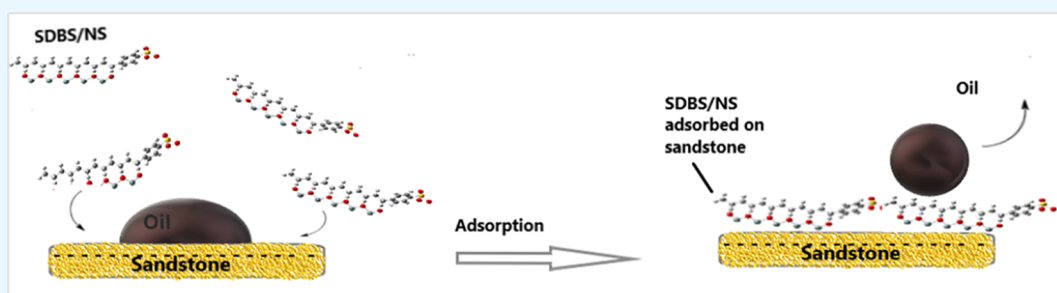George E. Azmi, Aya M. Saada, Eissa M. Shokir, Mohamed S. El-Deab,* Attia M. Attia,* and Walaa A. E. Omar*

Read Online

ACCESS | Metrics & More | Article Recommendations

ABSTRACT: Chemical flooding using a polymer and/or surfactant has been widely applied in oilfields worldwide for enhanced oil recovery. Chemical adsorption in reservoirs has a significant effect on the rock permeability and wettability and hence can affect the overall oil production. In this work, two chemicals, namely, the xanthan gum (XG) biopolymer and sodium dodecylbenzenesulfonate (SDBS) anionic surfactant, were used individually as displacement fluids. The amount of chemical adsorption on the rock surface and the residual resistance factor (permeability reduction) were calculated throughout the flooding experiments using an unconsolidated sandstone (SS) pack model. The effects of the injected chemicals' concentration and reservoir salinity on adsorption capacity have been examined. Additionally, the effect of the addition of nanosilica particles (NSPs) to the injected fluid on the rock adsorption was also investigated. The results showed that the amount of XG and SDBS adsorption on the rock surface increased, albeit to a different extent, by increasing the chemical concentration at the applied salinities (0, 3.5, 5, and 10%) of the displacement fluids. Also, the permeability reduction increased with the increase in XG and SDBS concentrations; however, permeability reduction due to SDBS flooding was lower than that of XG in SS. The use of NSPs as a coinjectant to the XG and SDBS displacement fluids increased the adsorption on the SS rock. A plausible mechanism for the adsorption of the XG/NSP and SDBS/NSP blends on the SS surface was proposed. A density function theory calculation was employed to establish a relation between the adsorptivity of NSPs on SDBS and XG and the total energy and dipole moment of the molecules.

1. INTRODUCTION

One of the main methods of tertiary oil recovery is chemical flooding, such as polymer and surfactant flooding. Understanding the effect of the salinity and the injected additives on the chemical adsorption in the reservoirs is essential to successful enhanced oil recovery (EOR) operations. Sandstone (SS) forms about 60% of the reservoir rock types around the world.[1] Polymer and anionic surfactant flooding are the most suitable and commonly used in SS reservoirs.[2]

Polymer flooding increases the oil recovery by increasing the injecting fluid viscosity and hence improving the oil mobility ratio and sweep efficiency.[3−7] Xanthan gum (XG) is the most widely reported biopolymer for oil applications.[2] Due to its chemical structure with the rigid polysaccharide chains (Figure 1), XG solution displays high thickening ability and good stability to the increasing temperature and salinity.[2] Moreover, the hydroxyl (−OH) and carboxyl (−COOH) polar groups of XG form intra- and intermolecular hydrogen bonds in aqueous solution. The viscosity of XG solutions caused by the hydrogen bonding, even at low concentrations, makes the polymer appropriate for polymer flooding in EOR.[3,5−8]
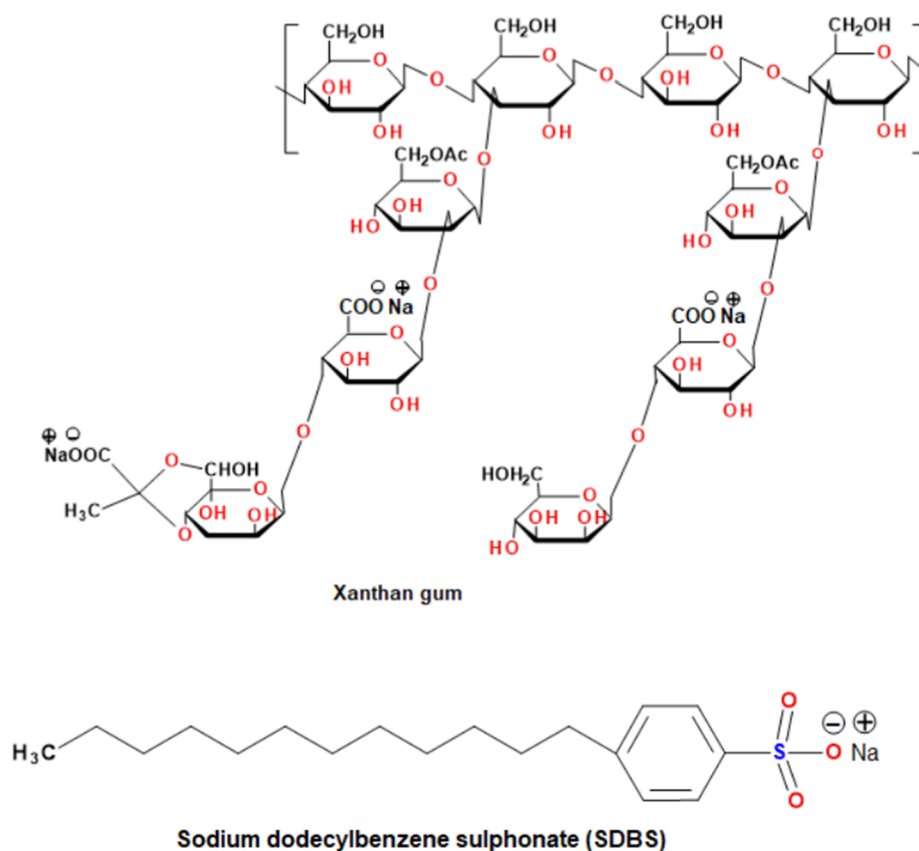
In surfactant flooding, the oil recovery increases by lowering the water/oil interfacial tension and wettability alteration.[9−12]

Figure 1. Chemical structure of XG and SDBS.

Sodium dodecylbenzenesulfonate (SDBS), shown in Figure 1, is an anionic surfactant that is widely used in EOR.[13] Anionic surfactants are most preferred for EOR, specifically with SS reservoirs.[14] It was observed that SDBS provided a high wettability change for quartz surface by an oil recovery factor of 93%.[15]

During polymer and surfactant flooding, the injected chemical molecules get adsorbed in the reservoir porous media, which affects the reservoir permeability and can cause a reduction in the recovered oil. Additionally, chemical adsorption in reservoirs decreases the effective concentration of the displacement fluid. As a result, an increase in the amount of the injected chemical is required to achieve the targeted recovery results.[16] On the other hand, in heterogeneous formations with different permeability zones, the polymer fluid preferably takes the high permeability path. Adsorption of the chemical and blockage in the high permeability zones are advantageous as they permit/allow the displacement fluid to reach the low permeability zones or the small pores and consequently enhance the sweep efficiency.[17] Similarly, the adsorption of the surfactant can have a positive effect on EOR. The adsorbed surfactant molecules on the rock surface alter the wettability of reservoir rock from oil wet to water wet, which is preferred for EOR.[16]

Therefore, for cost-effective chemical EOR, management and optimization of the chemical adsorption are mandatory.[16]

Zhu et al.[18] studied the effect of concentration on the adsorption of the synthetic polymer hydrolyzed polyacrylamide on the quartz surface. They reported that increasing the polymer concentration increased the amount of adsorption and that adsorption decreased with increasing fluid velocity.

In the same context, Ni et al.[19] studied the adsorption behavior of the anionic surfactant SDBS on the surface of montmorillonite minerals. They reported that the adsorption capacity increased with the increase in the concentration of SDBS. Surfactant adsorption in the reservoir was proved to be dependent on the nature of the surfactant and the rock surface. The interaction of the chemical and rock surface depends on the attraction forces that exist between the rock surface and functional groups on the polymer or surfactant chemical structure.[13,20]

Salt concentration (saline), temperature, and additives were also found to largely affect the adsorption capacity on the rock surface.[2,21] Additives such as nanoparticles have proved to enhance oil recovery remarkably.[22−25] Nanoparticles increase the viscosity of the injecting fluid and have the ability to change the wettability of the rock.[26] One of the recent trends in chemical flooding is the synergistic combination of nanoparticles and the chemical (polymer or surfactant) in the displacement fluid. That way, the injection fluid possessed the advantageous properties of both components, the polymer or surfactant and the nanoparticles,[2] that is, the rheological properties of the polymer increase in the presence of nanoparticles, and the nanoparticle stability also improved in the presence of the polymer solution.[13,27] Chen et al.[28] have used the density function theory (DFT) to calculate the adsorption energy to determine the stable adsorption configuration. Due to the high abundance of SS reservoirs compared to limestone,[29] in this paper, adsorption during XG and SDBS flooding on SS was fully investigated to boost their absorptivity for EOR. We also attempted to study the adsorption behavior of the biopolymer XG and the anionic

Scheme 1. Displacement Setup
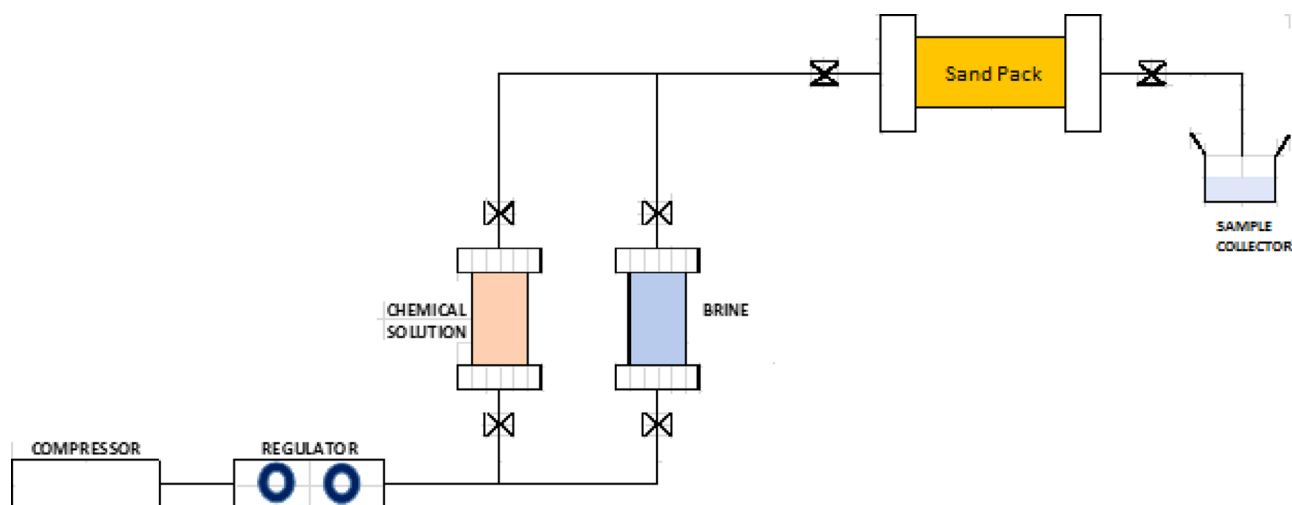
surfactant SDBS on SS reservoirs experimentally at different concentrations and salinities. The effect of the addition of nanosilica particles (NSPs) to the XG and SDBS displacement fluids was also studied at different concentrations. DFT calculations were employed to calculate the total energy and dipole moment of the XG/NSP and SDBS/NSP blends to predict the most stable adsorption configuration on the SS surface. The total energy of several binary combinations of XG or SDBS with NSPs is estimated and is taken as a probe to predict the most stable geometric configuration which is suitable for the adsorption on the SS surface. The marked increase in the dipole moment of XG or SDBS upon blending with NSPs is taken as a possible cause for the observed enhanced absorptivity. Based on the experimental results and the DFT calculations, plausible mechanisms for the adsorption of XG/NSPs and SDBS/NSPs on SS surfaces were proposed.

2. EXPERIMENTAL SECTION

2.1. Chemicals. The anionic surfactant, SDBS 80% extra pure, is purchased from Loba Chemie PVT. LTD (India). The XG Biopolymer and NSPs (hydrophilic) of size 20 nm were provided by ITA Co. (Egypt).

2.2. Displacement Apparatus. The schematic diagram of the displacement apparatus is shown in Scheme 1.[3] It consists of a sand pack with an inner diameter of 52 mm and a length of 210 mm. The model was fitted with two chambers in the inlet and the outlet to prevent the distribution effect and achieve uniform inlet and outlet distribution of the fluid. The inlet was connected to a regulator valve to measure the inlet pressure. The effluent fluid from the column was collected in a graduated glass cylinder. The same line was used to carry the injected fluids from two tanks: a chemical tank containing either the surfactant or polymer and a brine tank.

2.3. Displacement Procedures (Chemical Flooding). The sand pack was saturated with brine during the sand packing process, brine was then injected to calculate the permeability of the model before chemical injection;[3] then, the chemical (XG or SDBS) was injected to displace the brine, and samples of the chemical effluent were collected to determine its effluent concentration. Brine was then reinjected to displace the injected chemical, and permeability was measured once more to determine the residual resistance factor (R_{rf}), which is the ratio of the brine permeability before and after polymer

solution flows through the core.[30] All the chemical solutions were freshly prepared and continuously stirred before the experiments. Solutions were used as prepared; pH was not adjusted. A new sand pack was used for each experiment. Details of the sand pack are listed in Table 1.

Table 1. Sand Pack Properties

property, unit	value/unit
sand size, mm	0.3
length, cm	21
diameter, cm	5.2
area, cm^2	19.635
bulk volume, mL	412.334
pore volume, mL	100
porosity, %	25
permeability, mD	500−532

2.4. DFT Calculations. Gaussian G09 software was used to perform the DFT calculations to determine the total energy and dipole moment of SDBS and XG. The structures were drawn with initial geometries. Possible hydrogen bonds were suggested between XG or SDBS and NSPs. Then, a selected suitable basis set is chosen and allowed to run in the optimization mode to produce the optimum structures energetically and geometrically.

3. RESULTS AND DISCUSSION

3.1. Flooding Experiments and Adsorption Capacity Measurements. The effect of various operating parameters, namely, concentration, salinity, and NSPs as an additive on the adsorption capacity of XG and SDBS, has been investigated. After preparing the chemicals (either XG or SDBS), the viscosities were measured for the different concentrations. A calibration curve was then constructed between the influent concentrations, C_1, and the corresponding viscosities. After injecting the chemicals through the sand pack, effluent samples were collected, and their viscosities were measured. The measured effluent viscosities were then converted in concentrations, C_2, using the preconstructed calibration curves. The amount of adsorption (Ad) has been calculated (in mg/g-rock) using eq 1.[12,31] The R_{rf} has been calculated using eq 2.[32]

$$\text{Ad} = \frac{V}{M}(C_1 - C_2) \tag{1}$$

where V is the solution volume in L, M is the mass of sand in g m, C_1 is the influent concentration in ppm, and C_2 is the effluent concentration in mg/L. C_2 is calculated from the viscosity values.[33]

$$R_{rf} = \frac{K_{w1}}{K_{w2}} \tag{2}$$

where K_{w1} is the permeability of the model before chemical injection and K_{w2} is the permeability after chemical injection.

The XG concentrations applied for the adsorption experiments are 500, 1000, and 1500 ppm. For SDBS, the concentrations employed were 2000, 3000, and 5000 ppm. These concentrations are the typical polymer and surfactant dosages utilized in the industry.[9,34]

3.2. Adsorption of XG on the SS Rock. *3.2.1. Effect of Concentration and Salinity.* In Scheme 1, brine (3.5% NaCl) was first injected into the model followed by XG injection at a shear rate of 10 rounds per minute and salinity ranges of 0 to 10% to cover the possible average range of formation water in reservoirs. The injection procedures using the model in Scheme 1 were repeated at room temperature and using different XG concentrations, 500, 1000, and 1500 ppm. The concentrations have been selected according to the industrial doses frequently used.[9,31] Each of the aforementioned XG concentrations was injected at a salinity range of 3.5, 5, and 10%. The amount of adsorption and R_{rf} for all the carried experiments were calculated according to the equations prescribed in 1 and 2. The effect of both the parameters (concentration and salinity) on the adsorption capacity at room temperature has been summarized in Table 2.

Table 2. Adsorption Capacity and R_{rf} for XG on the SS Rock at Different Concentrations and Salinities at Room Temperature

	salinity 0%		
concentration (ppm)	500	1000	1500
adsorption (mg/g)	0.135	0.38	0.50
R_{rf}	2.0	2.56	2.78
	salinity 3.5%		
concentrations (ppm)	500	1000	1500
adsorption (mg/g)	0.18	0.41	0.55
R_{rf}	2.639	3.88	4.8
	salinity 5%		
concentration	500	1000	1500
adsorption	0.282	0.474	0.586
R_{rf}	3.569	4.545	5.128
	salinity 10%		
concentration	500	1000	1500
adsorption	0.322	0.555	0.720
R_{rf}	7.201	8.501	9.490

From Table 2, one can observe that at the same salinity, as the concentration of XG increased, the amount of adsorption and the R_{rf} values[35] increased. It was also observed that the rate of increase in the R_{rf} and the adsorption decrease as the chemical concentration increases, indicating that the adsorption may stabilize at high concentrations.

An explanation for the increase in the adsorption with the increased concentration can be attributed to the increase in the

availability of the XG molecules, which, by the way, got adsorbed on the rock surface. XG molecules are expected to be adsorbed on the rock surface through hydrogen bonds generated between the hydrogen of the hydroxyl groups in the polymer and the negatively charged SS surface.[17] The proposed mechanism for the adsorption of XG on the SS surface is illustrated in Figure 2a.

From Table 2, it can also be observed that for the same concentration, as the salinity increased from 0 to 10%, the adsorption capacity and the R_{rf} values increased. The increase in the adsorption and R_{rf} values when increasing the NaCl concentration can be attributed to the XG salting-out effect. The salting-out effect caused a decrease in the polymer solubility leading to XG precipitation and hence an increase in the adsorption.[36]

3.2.2. Effect of Addition of NSPs on the Adsorption during XG Flooding in SS Formation. The XG flooding experiments in the previous Section 3.2.1 were repeated after the addition of NSPs at three different concentrations (0.01, 0.1, and 0.2 wt %) to each concentration of XG at 0% salinity at room temperature. The overall adsorption capacity and R_{rf} were calculated using eqs 1 and 2, and the results are illustrated in Table 3.

From Table 3, it was observed that the addition of NSPs to the XG slug caused a monotonic increase in both the XG adsorption and the R_{rf} values. For instance, at the XG concentration of 500 ppm, as the concentration of the NSP additive increased from 0.01 to 0.2 wt %, the R_{rf} values increased from 2.6 to 23.8 (about 9 folds), respectively. The adsorption also increased, albeit to a smaller ratio, from 0.19 to 0.25 mg/g at the same conditions. It was also observed that the rate of increase in the R_{rf} values was remarkable for higher concentrations of NSPs such that at 1000 ppm of XG, the R_{rf} value increased by ≈ 11 folds when the NSP concentration increased from 0 to 0.01 wt %, while at the same concentration of XG, the R_{rf} value increased by ≈ 33 folds when the NSP concentration increased from 0.1 to 0.2 wt %.

The increase in the adsorption capacity by the addition of NSPs at 0% salinity can be attributed to adsorption of the NSP on the SS surface. This adsorption took place due to the formation of hydrogen bonds between the hydroxyl groups of the NSP[37,38] and the negatively charged SS surface.[39] The XG then got adsorbed on the silica adsorbed on the rock surface. A proposed mechanism for the adsorption of XG and NSP mixture is illustrated in Figure 2b.

Increasing the concentration of the NSPs increased the adsorption with the different XG concentrations. This increase in the overall adsorption is attributed to the availability of NSP particles, which may allow multilayer adsorption with NSPs acting as the cross linker between XG polymer chains through hydrogen bonds.[40,41]

3.3. Adsorption of SDBS on the SS Rock. In the flooding experiments of SDBS, the same procedure shown in Section 2.3 was followed. Brine (3.5% NaCl) was first injected in the model (Scheme 1) followed by SDBS injection at a shear rate 10 round per minute and salinity ranges from 0 to 10% to cover the possible average range of formation water in reservoirs. The injection procedures using the model in Scheme 1 were repeated at room temperature and using different SDBS concentrations, 2000, 3000, and 5000 ppm. eq 1 was implemented to calculate the adsorption capacity of SDBS on the SS for all the carried-out experiments. R_{rf} values were calculated using eq 2 (see Section 3.1).
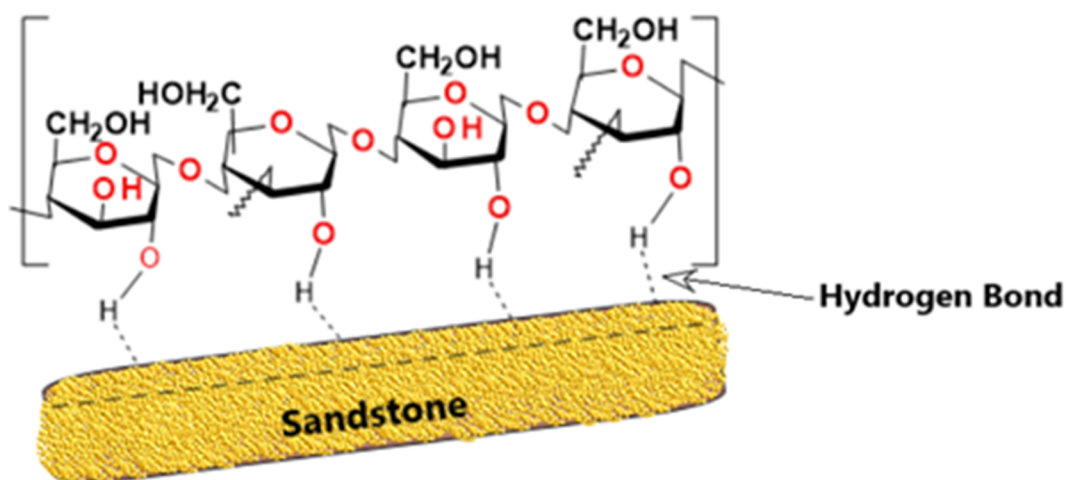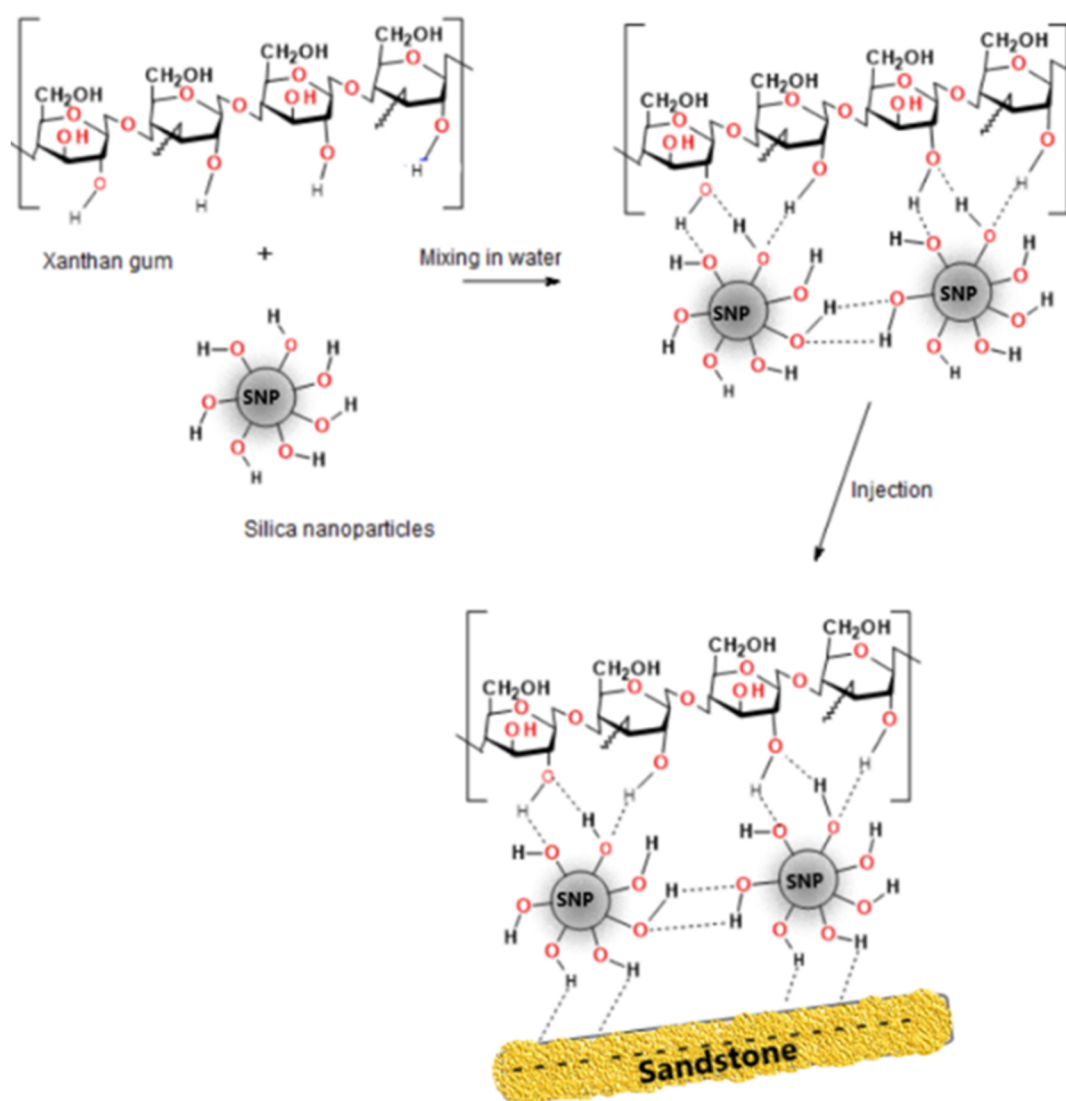
Figure 2. Proposed mechanism for the adsorption of XG on the SS surface (a) before the addition of NSPs and (b) in the presence of NSPs as an additive in deionized water.

Table 3. Adsorption Capacity and R_{rf} Values after the Addition of NSPs (0.01, 0.1, and 0.2 wt %) at 0% Salinity

	nanosilica 0.01%		
XG concentration (ppm)	500	1000	1500
adsorption (mg/g)	0.194	0.395	0.556
R_{rf}	2.60	11.555	24.073
	nanosilica 0.10%		
XG concentration (ppm)	500	1000	1500
adsorption (mg/g)	0.214	0.436	0.580
R_{rf}	10.639	22.502	38.271
	nanosilica 0.20%		
XG concentration (ppm)	500	1000	1500
adsorption	0.246	0.523	0.590
R_{rf}	23.804	55.192	74.799

3.3.1. Effect of Concentration and Salinity on the Adsorption Capacity and R_{rf} Values. The effect of changing the concentration of SDBS and salinity on the adsorption capacity and R_{rf} values during SDBS flooding in SS at room temperature has been summarized in Table 4.

Table 4. Effect of Concentration of SDBS and Salinity on the Adsorption Capacity and R_{rf} Values

	salinity 0%		
concentration of SDBS (ppm)	2000	3000	5000
adsorption (mg/g)	0.093	0.3561	0.545
R_{rf}	1.133	1.228	1.25
	salinity 3.5%		
concentration of SDBS (ppm)	2000	3000	5000
adsorption (mg/g)	0.2373	0.3654	0.6897
R_{rf}	1.212	1.533	1.671
	salinity 5%		
concentration of SDBS (ppm)	500	1000	1500
adsorption	0.333	0.495	0.786
R_{rf}	1.98	2.23	2.6
	salinity 10%		
concentration of SDBS (ppm)	2000	3000	5000
adsorption	0.47	0.74	0.93
R_{rf}	3.05	3.55	3.73

From Table 4, it was clear that as the concentration of the SDBS increased, the adsorption capacity and the R_{rf} values increased. The increase in the concentration of SDBS resulted in more availability of the SDBS molecules to be adsorbed on the SS surface. Also, as the salinity increased, the adsorption capacity and the R_{rf} values increased which is in agreement with data reported by Lee and Koopal.[42] This phenomenon can be explained as the existence of the salt ions reduced the repulsion between the ionic surfactant head and the negatively charged SS surface and hence increases the adsorption capacity.[43]

3.3.2. Effect of NSP Addition on the Adsorption and R_{rf} Values of SDBS at 0% Salinity. SDBS flooding in Section 3.3 was repeated using the same concentrations with the addition of NSPs at concentrations of 0.01, 0.1, and 0.2% for each SDBS concentration at 0% salinity. The results from the SDBS flooding after the addition of the different concentrations of NSPs are summarized in Table 5.

From Table 5, it is clear that, in general, the adsorption capacity increased with the addition of NSPs during the SDBS flooding in SS at the different concentrations and zero salinity. Additionally, as the concentration of the NSP additive

Table 5. Effect of the Addition of Different Concentrations of NSPs (0.01, 0.1, and 0.2 wt %) at 0% Salinity on the Adsorption Capacity and R_{rf} Values of SDBS in SS

|	nanosilica 0.01 wt %		
SDBS concentration (ppm)	2000	3000	5000
adsorption (mg/g)	0.47	0.57	0.93
R_{rf}	1.1	2.5	4.3
	nanosilica 0.10 wt %		
SDBS concentration (ppm)	2000	3000	5000
adsorption (mg/g)	0.6	0.9	1.1
R_{rf}	6.03	8.728	9.75
	nanosilica 0.20 wt %		
SDBS concentration (ppm)	2000	3000	5000
adsorption	0.708	1.0	1.296
R_{rf}	6.4	11	11.7

increased, the adsorption capacity and the R_{rf} values increased. Although the addition of NSPs increased the R_{rf} values during SDBS flooding, the values are much lower than those observed during XG/NSP flooding. A proposed mechanism for the adsorption of SDBS/NSPs on SS at 0% salinity is illustrated in Figure 3.

In Figure 3a, the negatively charged anionic surfactant heads point away from the negatively charged SS surface due to charge repulsion.[44] The anionic surfactant, SDBS, may approach the negatively charged SS surface more readily through the hydrophobic tail. The addition of NSPs (Figure 3b) increases the adsorption as the silica can form hydrogen bonds between the SS surface[45] and the hydrophobic tail (C–H bonds)[46,47] of the SDBS, resulting in attraction of more surfactant molecules to the SS surface.

3.4. DFT Calculations. The main objective of these calculations is to understand the different modes of interaction between NSPs and both chemicals, the SDBS surfactant, and XG during the flooding. This is done to establish a theoretical ground for the observed enhancement of NSPs toward the adsorptivity of the SDBS and XG (in the displacement fluids) onto the SS surface.

Gaussian 09 software was used to perform the DFT calculation employing the 3-21 G Basis set to determine the interaction of the NSP with XG and SDBS. For this purpose, the total energy and dipole moment of the SDBS/NSPs and XG/NSPs were calculated. The optimized structures of the XG and SDBS with and without NSPs are shown in Figure 4. Note that a selected negatively charged segment of XG is chosen for DFT calculations (Figure 4a) to resemble the negatively charged surfactant molecule. The outcomes of the DFT calculations are summarized in Table 6.

Inspection of Table 6 reveals that using NSPs (as a chain-like additive) together with SDBS boosted the stability of the XG segment and SDBS (as evident from the total negative energy shift). Moreover, the polarity of the SDBS/NSP blend is much higher (as evident by the dipole moment) than that of SDBS alone. As the dipole moment increases, the adsorptivity of SDBS/NSP or XG/NSP blends increases, leading to an increase in the rock water wettability.[48,49] An increase in the rock water wettability should repel oil away from the rock surface and enhance oil recovery. Thus, the proposed interaction between SDBS and NSPs (given above in Figure 3) could be reasonably considered to account for the observed adsorption behavior of the blend.
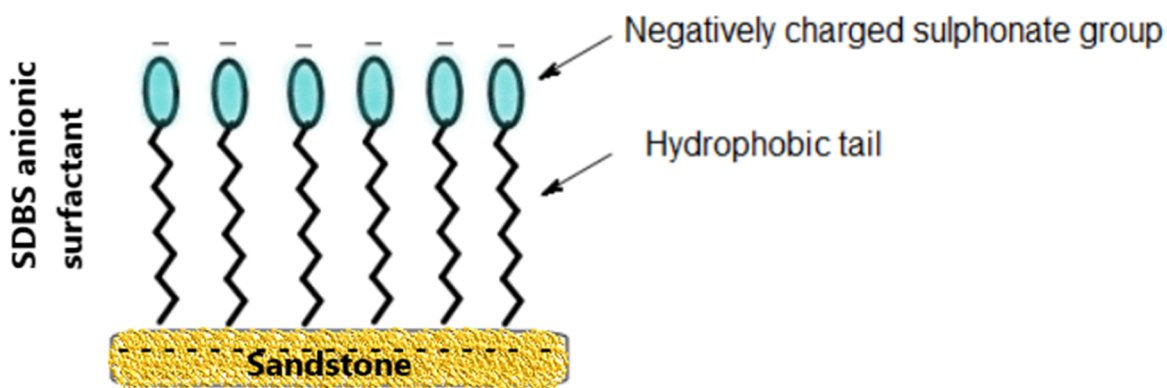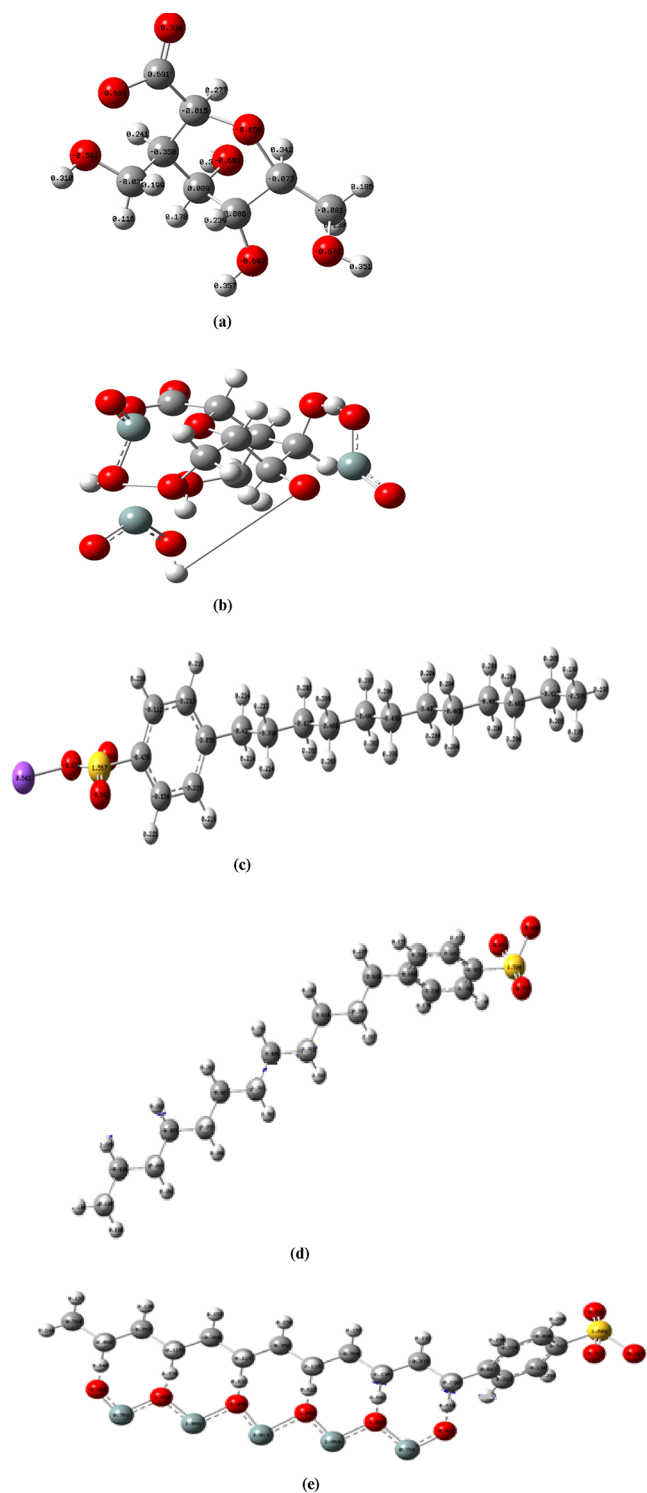
(a)
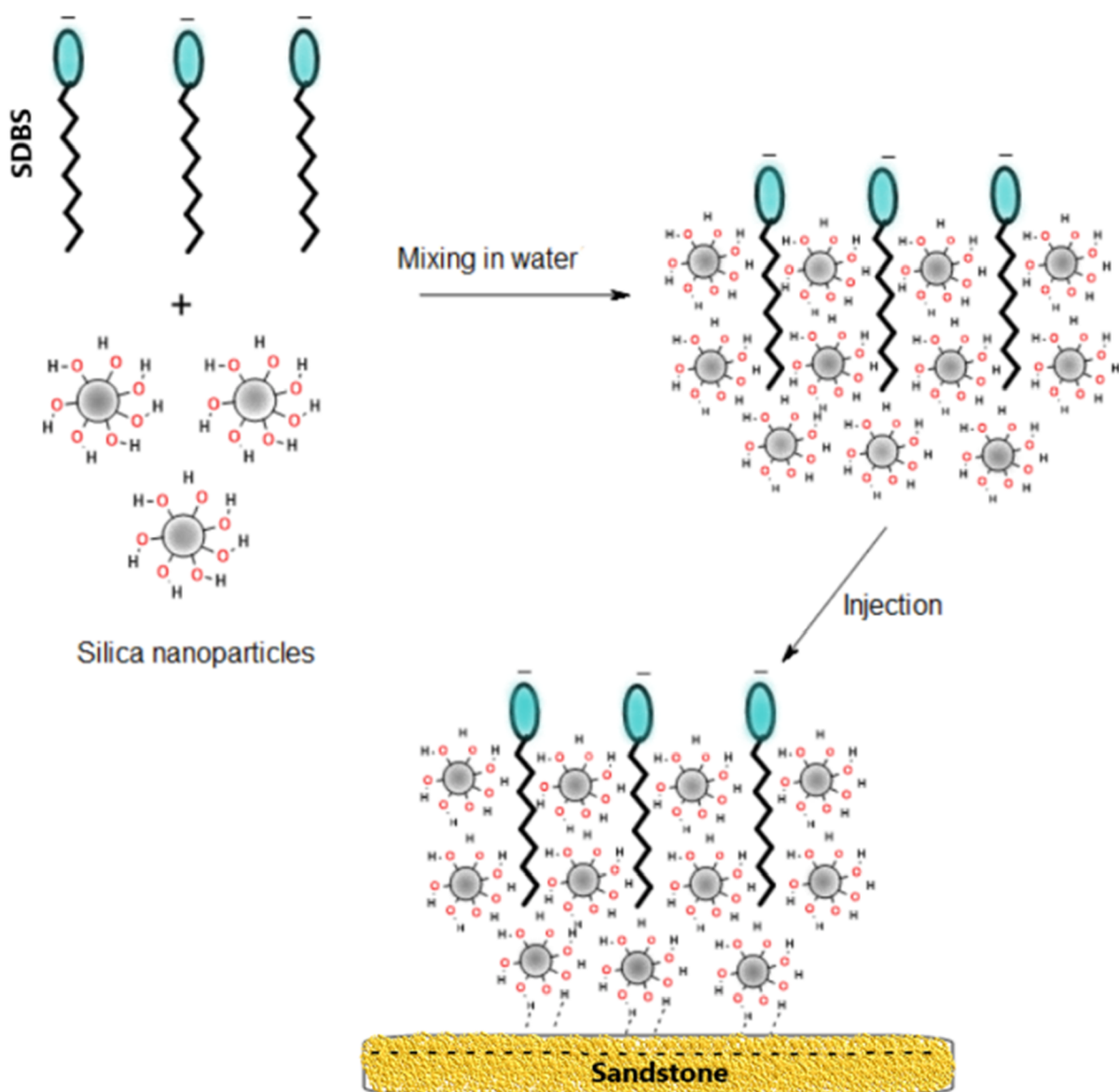
(b)

Figure 3. Proposed mechanism for the adsorption of the anionic surfactant SDBS on SS before the addition of NSPs and (b) after the addition of NSPs in deionized water.

(a)

(b)

(c)

(d)

(e)

Figure 4. DFT-optimized structure of the (a) XG polymer segment (II) carboxylate anion, (b) XG polymer segment (II) carboxylate anion—bonded to three SiO_2 molecules, (c) SDBS-salt, (d) SDBS anion, and (e) SDBS anion bound to the SiO_2 polymeric chain.

3.5. Adsorption and Enhancement of Oil Recovery.
The addition of NSPs improved the adsorption of both SDBS and XG on the SS rock grains. Hence, the NSP adsorption can improve the oil recovery in oil-wet rock. In the displacement fluids, the NSPs got bonded to XG and SDBS through hydrogen bonds.[42] Then, the SDBS/NSPs and XG/NSPs got adsorbed on the rock surface, resulting in an increase in the

Table 6. DFT Calculations for the Total Energy and Dipole Moment of the XG, SDBS, and XG/NSP and SDBS/NSP Structures Given in Figure 4

structure	total energy/hartree (a.e.u.)	dipole moment/debye
A	−829.9266	9.8008
b	−2139.2612	9.2854
c	−1473.4915	9.0191
d	−1312.6234	29.6116
e	−3195.6438	33.2546

rock water wettability.[50] Consequently, the oil should be repelled away from the SS surface. This chemical interpretation of the SDBS/NSP and XG/NSP interactions with the SS surface is strongly emphasized by the significant dipole moment evident from the DFT calculations. An illustration for the enhancement in oil recovery by adsorption on the surface through the NSP acting as a binder is represented in Figure 5. Although SDBS is used in the illustration, the same proposal is applicable to XG.

3.6. Enhancement Factor Calculations. To probe the enhancement in adsorptivity before and after the addition of NSPs, two parameters are calculated, the enhancement factor (EF) and the specific EF (SEF) using eqs 3 and 4, respectively. EF and SEF were calculated for XG and SDBS at 500 and 2000 ppm, respectively, and the data are summarized in Table 7.

$$EF = \frac{Ad \text{ in presence of additive}}{Ad \text{ in pure water}} \tag{3}$$

$$SEF = \frac{\text{enhancement factor}}{\text{mass of additive}} \tag{4}$$

From Table 7, one can conclude that (i) the solution salinity has a positive impact on the adsorptivity of XG and SDBS, that is, about a two- to three-fold increase in the amount of adsorbed XG and SDBS, respectively, in a 5% saline solution compared to pure water. This is in agreement with the data reported by Belhaj et al.[43] (ii) The influence of salinity on SDBS adsorption is more pronounced than that on XG; (iii) NSP addition showed a positive impact on the adsorptivity of both XG and SDBS; (iv) the sensitivity of SDBS adsorption to NSP addition is more significant than that of XG (compare the EF values in the absence and the presence of NSPs and refer to the DFT calculations given above); (v) the addition of a minute amount of NSPs caused a remarkable rise in SEF values compared to the impact of salinity; (vi) increased amounts of NSPs showed a less pronounced effect on EF for both XG and SDBS. Thus, one can argue that the proposed system of the SDBS/NSP blend would have a positive impact on the improved water wettability of SS rocks and could be used for effective EOR systems with the use of minute amounts of NSPs, as small as 0.01%, together with 0.2 wt % of the SDBS surfactant.

4. CONCLUSIONS

Based on the experimental results of this work, the following conclusions can be reached:

(1) When increasing the chemical concentration of NSP, the amount of adsorption on the rock surface increases; however, it was found that the effect is more profound in the case of the XG polymer.
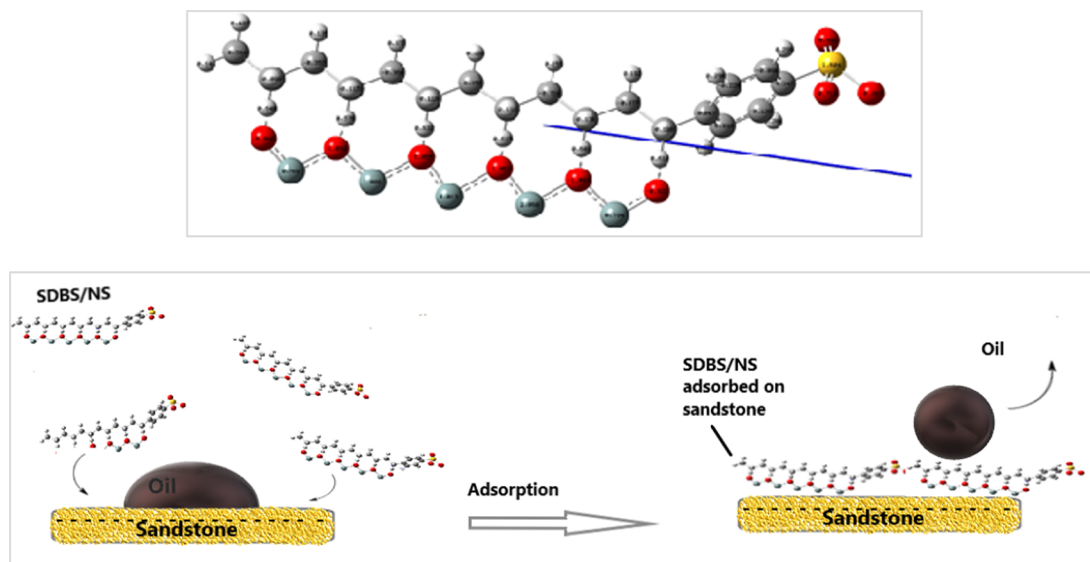
Figure 5. Top: The anionic surfactant−SiO$_2$−polymeric chain with the dipole moment direction (dipole moment = 33.2546 debye). Below: Possible mechanism for SDBS/NSP adsorption on SS that enhances oil recovery through increased water wettability.

Table 7. Calculated EF and SEF for XG and SDBS before and after NSP Addition

displacement fluid	XG (500 ppm)				SDBS (2000 ppm)			
salinity %	0	3.5	5	10	0	3.5	5	10
EF	1	1.33	2.08	2.39	1	2.55	3.58	5.05
SEF		0.38	0.417	0.238		0.728	0.716	0.205
displacement fluid	XG (500 ppm)				SDBS (2000 ppm)			
salinity %	0				0			
nanosilica conc. wt %	0.01	0.1	0.2		0.01	0.1	0.2	
EF	1.437	1.580	1.812		5.05	6.45	7.61	
SEF	143.7	15.8	9.06		505	64.5	38.5	

(2) NSP increases the adsorptivity of SDBS or XG and thus alters the SS rock to be more water-wet rather than oil-wet.

(3) The proposed system of the SDBS/NSP blend would have a positive impact on the improved water wettability of SS rocks and could be used for effective EOR systems with the use of minute amounts of NSPs, as small as 0.01%, together with 0.2 wt % of the SDBS surfactant.

(4) Both the R_{rf} and the amount of chemical adsorption increase by increasing the formation water salinity for the XG and SDBS flooding, and it was also observed that the amount of adsorption increasing due to salinity is greater in the case of XG flooding.

(5) DFT calculations provide a theoretical ground for the explanation of the observed enhanced adsorptivity given the obtained quantum chemical parameters, for example, total energy and dipole moment of the various blends with NSP. The authors acknowledge The British University in Egypt (BUE), Petroleum Engineering and Gas Technology Department, for funding this research and for providing the necessary facilities.

■ AUTHOR INFORMATION

Corresponding Authors

Mohamed S. El-Deab − *Department of Chemistry, Faculty of Science, Cairo University, Cairo 12613, Egypt;* orcid.org/0000-0001-9089-3399; Email: msaada@cu.edu.eg

Attia M. Attia − *Faculty of Energy and Environmental Engineering (FEEE), The British University in Egypt, Cairo 11837, Egypt;* Email: attia.attia@bue.edu.eg

Walaa A. E. Omar − *Faculty of Energy and Environmental Engineering (FEEE), The British University in Egypt, Cairo 11837, Egypt; Department of Engineering Sciences and Mathematics, Faculty of Petroleum and Mining Engineering, Suez University, Suez 8151650, Egypt;* orcid.org/0000-0002-2115-4469; Email: walaa.omar@bue.edu.eg

Authors

George E. Azmi − *Faculty of Energy and Environmental Engineering (FEEE), The British University in Egypt, Cairo 11837, Egypt*

Aya M. Saada − *Faculty of Energy and Environmental Engineering (FEEE), The British University in Egypt, Cairo 11837, Egypt*

Eissa M. Shokir − *Gas Production Engineering Department, Faculty of Engineering, Cairo University, Cairo 12613, Egypt;* orcid.org/0000-0002-7623-9646

Complete contact information is available at:
https://pubs.acs.org/10.1021/acsomega.2c03488

Notes

The authors declare no competing financial interest.

■ REFERENCES

(1) Knebel, G. M.; Rodriguez-Eraso, G. Habitat of Some Oil. *AAPG Bull.* **1956**, *40*, 547−561. https://archives.datapages.com/data/bulletns/1953-56/images/pg/00400004/0750/07890.pdf

(2) Gbadamosi, A. O.; Junin, R.; Manan, M. A.; Agi, A.; Yusuff, A. S. An overview of chemical enhanced oil recovery: recent advances and aspects. *Int. Nano Lett.* **2019**, *9*, 171−202.

(3) Elsaeed, S. M.; Zaki, E. G.; Omar, W. A. E.; Ashraf Soliman, A. A.; Attia, A. M. Guar Gum-Based Hydrogels as Potent Green Polymers for Enhanced Oil Recovery in High-Salinity Reservoirs. *ACS Omega* **2021**, *6*, 23421−23431.

(4) El-hoshoudy, A. N.; Gomaa, S.; Hassan, A.; Attia, A. M. Effects of alkaline/polymer/nanofluids on oil recovery at harsh reservoir conditions. *J. Pet. Sci. Eng.* **2019**, *181*, 106236 https://www.vurup.sk/wp-content/uploads/2019/12/PC-X-2019_El-hoshoudy-141_rev3.pdf.

(5) An, A. N.; El Desouky, S. M.; Attia, A. M.; Gomaa, S. Synthesis and Evaluation of Xanthan-G-Poly (Acrylamide) Co-Polymer for Enhanced Oil Recovery Applications. *Pet. Petro. Chem. Eng. J.* **2018**, *2*, 1−8.

(6) Patel, J.; Maji, B.; Moorthy, N. S. H. N.; Maiti, S. Xanthan Gum Derivatives: Review of Synthesis, Properties and Diverse Applications. *RSC Adv.* **2020**, *10*, 27103−27136.

(7) Mahran, S.; Attia, A. M.; Saha, B. A Review on Polymer Flooding in Enhanced Oil Recovery Under Harsh Conditions. *Proceedings of SEEP*, 2018; pp 1−6. https://openresearch.lsbu.ac.uk/item/86qz2.

(8) Ashraf Soliman, A. A.; El-hoshoudy, A. N.; Attia, A. M. Assessment of xanthan gum and xanthan-g-silica derivatives as chemical flooding agents and rock wettability modifiers. *Oil Gas Sci. Technol.—Rev. IFP Energies nouvelles* **2020**, *75*, 12−13.

(9) Massarweh, O.; Abushaikha, A. S. The Use of Surfactants in Enhanced Oil Recovery: A Review of Recent Advances. *Energy Rep.* **2020**, *6*, 3150−3178.

(10) Kalam, S.; Abu-Khamsin, S. A.; Kamal, M. S.; Patil, S. A review on surfactant retention on rocks: mechanisms, measurements, and influencing factors. *Fuel* **2021**, *293*, 120459.

(11) Kalam, S.; Abu-Khamsin, S. A.; Kamal, M. S.; Patil, S. Surfactant Adsorption Isotherms: A Review. *ACS Omega* **2021**, *6*, 32342−32348.

(12) Kalam, S.; Abu-Khamsin, S. A.; Kamal, M. S.; Hussain, S. M. S.; Norrman, K.; Mahmoud, M.; Patil, S. Adsorption Mechanisms of a Novel Cationic Gemini Surfactant onto Different Rocks. *Energy Fuels* **2022**, *36*, 5737−5748.

(13) Ngo, I.; Srisuriyachai, F.; Sasaki, K.; Sugai, Y.; Nguele, R. Effects of Reversibility on Enhanced Oil Recovery Using Sodium Dodecylbenzene Sulfonate (SDBS). *J. Jpn. Pet. Inst.* **2019**, *62*, 188−198.

(14) Isaac, O. T.; Pu, H.; Oni, B. A.; Samson, F. A. Surfactants employed in conventional and unconventional reservoirs for enhanced oil recovery—A review. *Energy Rep.* **2022**, *8*, 2806−2830.

(15) Esfandyari, H.; Shadizadeh, S. R.; Esmaeilzadeh, F.; Davarpanah, A. Implication of anionic and natural surfactants to measure wettability alteration in EOR processes. *Fuel* **2020**, *278*, 118392−118398.

(16) Shoaib, M.; Quadri, S. M. R.; Wani, O. B.; Bobicki, E.; Garrido, G. I.; Elkamel, A.; Abdala, A. Adsorption of enhanced oil recovery polymer, schizophyllan, over carbonate minerals. *Carbohydr. Polym.* **2020**, *240*, 116263−116270.

(17) Kumar, A.; Mandal, A. Critical investigation of zwitterionic surfactant for enhanced oil recovery from both sandstone and carbonate reservoirs: Adsorption, wettability alteration and imbibition studies. *Chem. Eng. Sci.* **2019**, *209*, 115222.

(18) Zhu, S.; Ye, Z.; Liu, Z.; Chen, Z.; Li, J.; Xiang, Z. Adsorption characteristics of polymer solutions on media surfaces and their main influencing factors. *Polymers* **2021**, *13*, 1774.

(19) Ni, X.; Li, Z.; Wang, Y. Adsorption Characteristics of Anionic Surfactant Sodium Dodecylbenzene Sulfonate on the Surface of Montmorillonite Minerals. *Front. Chem.* **2018**, *6*, 1−10.

(20) Sayyouh, M. H.; Al-Blehed, M. S.; Attia, A. M. The Effect of Alkaline and Polymer Additives on Phase Behaviour of Surfactant-Oil-Brine System at High Salinity Conditions. *Oil & Gas Science and Technology - Rev. IFP* **1993**, *48*, 359−369.

(21) Attia, A. M.; Musa, H. Effect of Sodium Magnesium Silicate Nanoparticles on Rheology of Xanthan Gum Polymer. *Int. J. Eng. Sci.* **2015**, *6*, 1349. https://www.ijser.org/paper/Effect-of-Sodium-Magnesium-Silicate-Nanoparticles-on-Rheology-of-Xanthan-Gum-Polymer.html

(22) Mohajeri, M.; Hemmati, M.; Shekarabi, A. S. An Experimental Study on using a nanosurfactant in an EOR process of heavy oil in fractured micromodel. *J. Pet. Sci. Eng.* **2015**, *126*, 162−173.

(23) Abdelfatah, E.; Kang, K.; Pournik, M.; Shiau, B. J. B.; Harwell, J. Mechanistic study of nanoparticles deposition and release in porous media. *J. Pet. Sci. Eng.* **2017**, *157*, 816−832.

(24) Abdelfatah, E.; Pournik, M.; Shiau, B. J. B.; Harwell, J. Mathematical modeling and simulation of nanoparticles transport in heterogeneous porous media. *J. Nat. Gas Sci. Eng.* **2017**, *40*, 1−16.

(25) Abdelfatah, E.; Pournik, B. J. B.; Shiau, J. *Mathematical Modeling and Simulation of Formation Damage Associated with Nanoparticles Transport in Porous Media.* SPE-184894-MS, 2017; pp 1−11.

(26) Eltoum, H.; Yang, Y.-L.; Hou, J.-R. The effect of nanoparticles on reservoir wettability alteration: a critical review. *Pet. Sci.* **2021**, *18*, 136−153.

(27) Hu, Z.; Haruna, M.; Gao, H.; Nourafkan, E.; Wen, D. Rheological Properties of Partially Hydrolyzed Polyacrylamide Seeded by Nanoparticles. *Ind. Eng. Chem. Res.* **2017**, *56*, 3456−3463.

(28) Chen, Y.; Xu, D.; Zhang, S.; Tan, R.; Li, L.; Liu, X.-Y. Density functional theory calculations on the adsorption and degradation characteristics of ronidazole on the TiO_2 surface. *Int. J. Quantum Chem.* **2021**, *121*, No. e26648.

(29) Bjørlykke, K.; Jahren, J. Sandstone and sandstone reservoirs. *Pet. Geosci.* **2010**, 113−140.

(30) Wang, C.; Liu, P.; Wang, Y.; Yuan, Z.; Xu, Z. Experimental Study of Key Effect Factors and Simulation on Oil Displacement Efficiency for a Novel Modified Polymer BD-HMHEC. *Sci. Rep.* **2018**, *8*, 3860.

(31) Tay, A.; Okhemanou, F.; Wartenberg, N.; Moreau, p.; Guillon, V.; DelbosTabary, A. R. Adsorption inhibitors: a new route to mitigate adsorption in chemical enhanced oil recovery. *SPE Enhanced Oil Recovery Conference*, SPE-174603-MS, 2015.

(32) Stahl, G. A.; Moradi-Araghi, A.; Doe, P. H. High Temperature and Hardness Stable Copolymers of Vinylpyrrolidone and Acrylamide. *Water-Soluble Polymers for Petroleum Recovery*; Springer Science Business Media: New York, 1988; pp 121−130.

(33) Lam, C.; Martin, P. J.; Jefferis, S. A.; Goodhue, K. G., Jr. Determination of Residual Concentration of Active Polymer in a Polymeric Support Fluid. *Geotech. Test. J.* **2014**, *37*, 46−59.

(34) Coolman, T.; Alexander, D.; Maharaj, R.; Soroush, M. An evaluation of the enhanced oil recovery potential of the xanthan gum and aquagel in a heavy oil reservoir in Trinidad. *J. Pet. Explor. Prod. Technol.* **2020**, *10*, 3779−3789.

(35) Mishra, S.; Bera, A.; Mandal, A. Effect of Polymer Adsorption on Permeability Reduction in Enhanced Oil Recovery. *J. Pet. Eng.* **2014**, *2014*, 395857.

(36) Braga, A. L. M.; Azevedo, A.; Julia Marques, M. J.; Menossi, M.; Cunha, R. L. Interactions between soy protein isolate and xanthan in heat-induced gels: The effect of salt addition. *Food Hydrocoll* **2006**, *20*, 1178−1189.

(37) Li, S.; Lau, H. C.; Torsæter, L.; Hendraningrat, C.; Temizel, C. Nanoparticles for enhanced oil recovery. *Sustain. Mater. Oil Gas Appl.* **2021**, *1*, 125−174.

(38) Xie, Q.; Hao, T.; Zhang, J.; Wang, C.; Zhang, R.; Qi, H. Anti-Icing Performance of a Coating Based on Nano/Microsilica Particle-Filled Amino-Terminated PDMS-Modified Epoxy. *Coatings* **2019**, *9*, 771.

(39) Bracho, D.; Dougnac, V. N.; Palza, H.; Quijada, R. Functionalization of Silica Nanoparticles for Polypropylene Nanocomposite Applications. *J. Nanomater.* **2012**, *2012*, 1−8.

(40) Potanin, A. Rheology of silica dispersions stabilized by polymers. *Colloids surf. A* **2019**, *562*, 54−60.

(41) Nassau, K.; Raghavachari, K. Hydrogen bonding consideration in silica gels. *J. Non Cryst. Solids* **1988**, *104*, 181−189.

(42) Lee, E. M.; Koopal, L. K. Adsorption of cationic and anionic surfactants on metal oxide surfaces. *J. Colloid Interface Sci.* **1996**, *177*, 478−489.

(43) Belhaj, A. F.; Elraies, K. A.; Mahmood, S. M.; Zulkifli, N. N.; Akbari, S.; Hussien, O. S. The effect of surfactant concentration, salinity, temperature, and pH on surfactant adsorption for chemical enhanced oil recovery: a review. *J. Pet. Explor. Prod. Technol.* **2020**, *10*, 125−137.

(44) Mohd, T. A. T.; Jaafar, M. Z. Adsorption of anionic sodium dodecyl sulphate surfactant on local sand and kaolinite surfaces: The prospect of alkaline and salinity. *Int. J. Recent Technol. Eng.* **2019**, *7*, 972−979. http://eprints.utm.my/id/eprint/90306/

(45) Ahmadi, M. A.; Shadizadeh, S. R. Induced effect of adding nanosilica on adsorption of a natural surfactant on sandstone rock: Experimental and theoretical studies. *J. petrol. Sci. Eng.* **2013**, *112*, 239−247.

(46) Li, Q.; An, X.; Gong, B.; Cheng, J. Cooperativity between OH...O and CH...O hydrogen bonds involving sulfoxide-H_2O-H_2O complex. *J. Phys. Chem. A* **2007**, *111*, 10166−10169.

(47) Sarkhel, S.; Desiraju, G. R. N-H...O, O-H...O, and C-H...O hydrogen bonds in protein-ligand complexes: strong and weak interactions in molecular recognition. *Proteins* **2004**, *54*, 247−259.

(48) Vijayakumar, S.; Kolandaivel, P. Study of static dipole polarizabilities, dipole moments, and chemical hardness for linear CH3−(CbC)n−X (XZH, F, Cl, Br, and NO_2 and nZ1−4) molecules. *J. Mol. Struc.-Theochem.* **2006**, *770*, 23−30.

(49) Li, X.; Deng, S.; Fu, H. Adsorption and inhibition effect of vanillin on cold rolled steel in 3.0 M H_3PO_4. *Prog. Org. Coat.* **2010**, *67*, 420−426.

(50) Li, S.; Kaasa, A. T.; Hendraningrat, L.; Torsaeter, O. Effect of Silica Nanoparticles Adsorption on the Wettability Index of Berea Sandstone. *International Symposium of the Society of Core*, 2013; pp1−7.